Traffic

Published by John Wiley & Sons Ltd
doi:10.1111/tra.12157

Regulated Oligomerization Induces Uptake of a Membrane Protein into COPII Vesicles Independent of Its Cytosolic Tail

Sebastian Springer[1,*], Per Malkus[2], Britta Borchert[1], Ursula Wellbrock[1], Rainer Duden[3] and Randy Schekman[4]

[1]Biochemistry and Cell Biology, Jacobs University Bremen, Bremen, Germany
[2]Department of Systems Biology, Harvard Medical School, Boston, MA 02115, USA
[3]Centre for Structural and Cell Biology in Medicine, Institute of Biology, University of Lübeck, Lübeck, Germany
[4]Howard Hughes Medical Institute and Department of Molecular and Cell Biology, University of California, Berkeley, Berkeley, CA 94720, USA
*Corresponding author: Sebastian Springer, s.springer@jacobs-university.de

Abstract

Export of transmembrane proteins from the endoplasmic reticulum (ER) is driven by directed incorporation into coat protein complex II (COPII)-coated vesicles. The sorting of some cargo proteins into COPII vesicles was shown to be mediated by specific interactions between transmembrane and COPII-coat-forming proteins. But even though some signals for ER exit have been identified on the cytosolic domains of membrane proteins, the general signaling and sorting mechanisms of ER export are still poorly understood. To investigate the role of cargo protein oligomer formation in the export process, we have created a transmembrane fusion protein that – owing to its FK506-binding protein domains – can be oligomerized in isolated membranes by addition of a small-molecule dimerizer. Packaging of the fusion protein into COPII vesicles is strongly enhanced in the presence of the dimerizer, demonstrating that the oligomeric state is an ER export signal for this membrane protein. Surprisingly, the cytosolic tail is not required for this oligomerization-dependent effect on protein sorting. Thus, an alternative mechanism, such as membrane bending, must account for ER export of the fusion protein.

Keywords ER export, *in vitro* COPII vesicle generation assay, membrane bending, oligomerization, transmembrane protein

Received 29 July 2013, revised and accepted for publication 7 January 2014, uncorrected manuscript published online 30 January 2014, published online 25 February 2014

In eukaryotic cells, transmembrane proteins destined for the secretory pathway or the plasma membrane are first inserted into the endoplasmic reticulum (ER). From there, they travel to the Golgi apparatus in membrane vesicles covered with the coat protein complex II (COPII) coat (1–3), which minimally comprises five proteins: the small GTPase Sar1 and the two protein complexes Sec23/24 and Sec13/31. Upon activation by guanosine triphosphate (GTP) binding, Sar1 recruits Sec23/24 to the ER membrane; it then interacts with Sec13/31, directing it to the membrane. Sec13/31 polymerizes the COPII coat and composes the outermost layer of the emerging vesicle (4–7).

Protein transport out of the ER was initially proposed to be non-selective, with ER-resident proteins maintaining their steady-state distribution via selective retrieval (6,8–10). However, quantitative comparison of the contents of COPII-coated vesicles to those of the ER membranes revealed that many cargo proteins were highly enriched in the vesicles (11,12). Amino acid motifs required for concentrative packaging have been identified in the sequence of several cargo proteins, as have the specific interactions between these motifs and components of the COPII coat (13,14). Additional studies have identified transmembrane receptor proteins that link soluble cargo proteins in the lumen of the ER to the cytosolic coat

proteins (15). Large cargo proteins (e.g. collagen), which do not fit in a standard COPII vesicle, need additional coat-binding or -regulating proteins (e.g. TANGO1, cTAGE5 and Sedlin) to be incorporated (6,16–19). Thus, uptake into COPII vesicles employs a specific sorting and concentration process *in vitro* and *in vivo* (20–22), and direct protein–protein binding interactions provide one compelling mechanism for mediating protein sorting in the ER.

To date, the majority of work has focused on the signal-mediated interactions of cargo proteins with the COPII coat that direct cargo into COPII vesicles (13,23–28). Cargo proteins can directly interact with one of three binding sites on the COPII coat component, Sec24, with an additional site in the human C and D isoforms (29–33). Several Sec24-binding motifs have been discovered on a variety of eukaryotic membrane proteins including dihydrophobic (13,34), diacidic (26,35), triple arginine (36) and aromatic motifs (25,26).

The majority of ER-exported membrane proteins, however, carry no known export signal in their sequence (6,27). Thus, either new signals remain to be identified or something else drives their recruitment into COPII vesicles. As many membrane proteins form oligomers prior to export from the ER (37), combinatorial signals (i.e. oligomeric signals composed from many weakly interacting sequences) have been postulated to link oligomerization to efficient export (27). Indeed, for a yeast COPII-binding cargo receptor protein and its mammalian homolog, oligomerization is required for its export from the ER (38,39).

In this article, we report the construction of a model transmembrane fusion protein that can be oligomerized in isolated microsomal membranes by a chemical dimerizer. We find that uptake of the oligomerized protein into COPII vesicles *in vitro* is strongly enhanced and independent of the cytosolic domain. Apparently, the oligomeric status of a membrane protein alone can promote its exit from the ER independent of any known export signal. We propose that protein oligomerization can generate a local membrane curvature that promotes vesicle formation, and thus the oligomeric form is preferentially packaged into transport vesicles without direct protein–protein binding interactions.

Results

A membrane protein for regulated oligomerization

To avoid interference with cellular processes, we used in the construction of our fusion protein a mutant drug-binding domain of the FK506-binding protein, FKBP(F36V) (40), which binds the dimerizer reagent, AP20187. This dimerizer does not interact with any endogenous FKBP in yeast (41,42). The fusion construct, named *F*KBP-*T*MD-*FF*, or FT-FF for short, contained the following domains (Figure 1A): the promoter and signal sequence of carboxypeptidase Y (CPY, *PRC1*) (43), a double influenza hemagglutinin (HA_2) tag for antibody-based detection, a target site for N-linked glycosylation, two FKBP(F36V) domains, the transmembrane domain (TMD) from *WBP1* (44,45) and a short cytosolic domain corresponding to the C-terminal 13 amino acids of the Prm8 protein. Prm8 (YGL053W) is a plasma membrane protein that may be involved in cell fusion during mating (46–48). The Prm8 sequence (YWRQEYPGVDEFF) was chosen because it contains two postulated ER exit motifs (13) and because preliminary experiments demonstrated that it bound to the Sec23/24 complex of COPII. We used two FKBP domains because previous experience suggested that a single FKBP domain might fail to cause efficient dimerization of a transmembrane protein (49).

Expression of the FT-FF gene in yeast cells and analysis by SDS–PAGE and immunoblotting resulted in a doublet of bands at approximately 32 and 35 kDa. Both forms of the protein were extractable from a membrane fraction by Triton X-100 and not by urea or sodium carbonate, suggesting that they are transmembrane proteins (Figure 1B). Treatment with Endoglycosidase H (EndoH) resulted in a single species running at 32 kDa, indicating that only the upper band was N-glycosylated (Figure 1C). As the lower band had the same apparent molecular weight as the deglycosylated upper band (Figure 1C), we concluded that the lower band was probably incorrectly inserted into the membrane, most likely in an inverse (type II) orientation. For additional confirmation, we performed proteinase K treatment of intact microsomal membranes, which resulted in preferential degradation of the lower band protein, supporting our conclusion that its N-terminal domain faces the cytosol (Figure 1D). The slight protease sensitivity

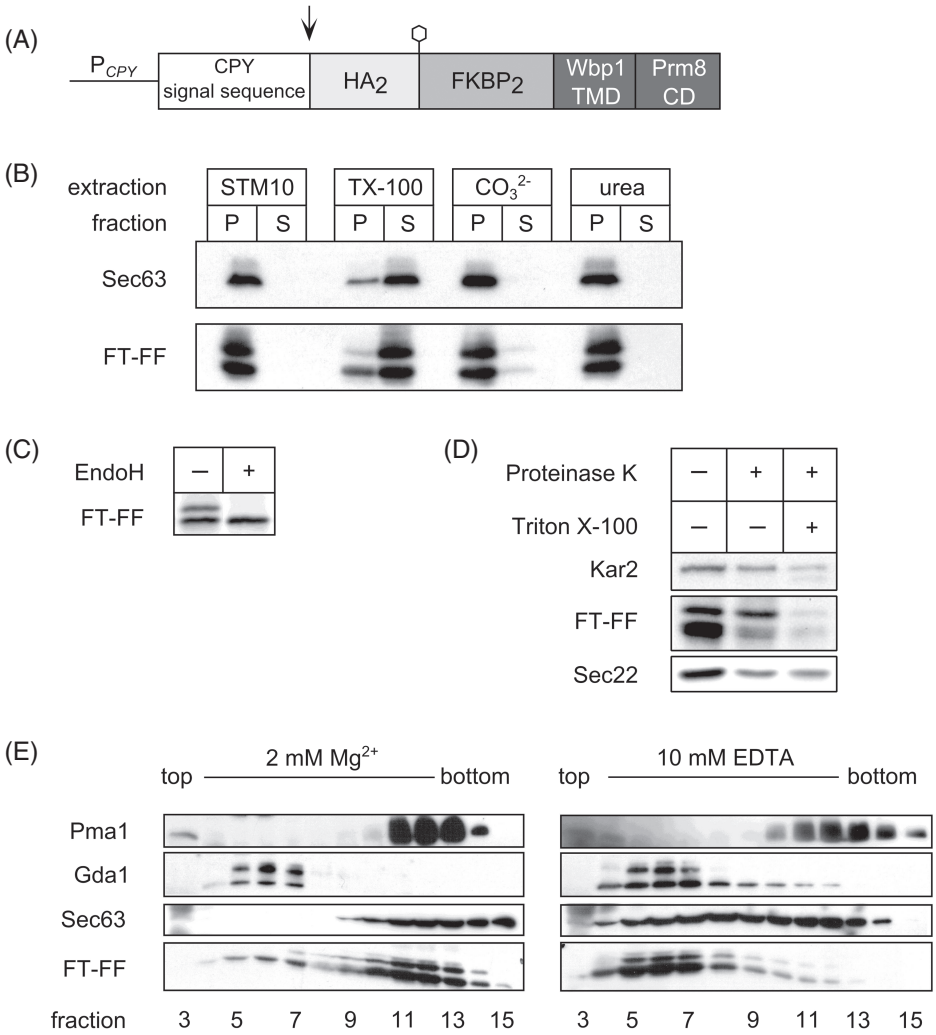

Figure 1: Design and biochemical characterization of the protein dimerization construct, FT-FF. A) Design of the FT-FF construct. Line, promoter region; box, protein coding region. P_{CPY}, CPY promoter; $FKBP_2$, two sequential FK506 (F36V)-binding protein domains; hexagon, glycosylation site in the protein; HA_2, two sequential influenza hemagglutinin epitope tags; TMD, transmembrane domain; CD, cytosolic domain. The asterisk indicates cleavage by signal peptidase in the ER. B) FT-FF is a transmembrane protein and appears in two forms. Detergent, carbonate and urea extraction from microsomes. S, supernatant; P, pellet. STM10, extraction with lysis buffer. TX-100, Triton buffer (1% Triton X-100 in 150 mM NaCl and 10 mM Tris–Cl), pH 7.5; CO_3^{2-}, 100 mM Na_2CO_3; urea, 2.5 M urea in 10 mM Tris–Cl, pH 7.5; Sec63, ER transmembrane control protein. Proteins were detected by immunoblotting. C) Only the upper band is glycosylated. FT-FF was immunoprecipitated with anti-HA antibodies from lysates of radiolabeled cells and then treated with EndoH. Only the upper band is sensitive to the enzyme and therefore glycosylated. The smaller amount of protein in the EndoH-treated lane may result from degradation during the overnight incubation. D) Only the upper band of FT-FF is protease-resistant. Microsomes were treated with 5 μg/mL proteinase K in the presence or absence of detergent as indicated, and the proteins were detected by SDS–PAGE and immunoblotting. Like Kar2, an ER lumenal chaperone, the upper band of FT-FF is resistant to proteinase K, and therefore correctly inserted into the membranes. The *N*-ethylmaleimide-sensitive-factor attachment receptor (SNARE) Sec22 only shows partial proteinase K sensitivity. E) FT-FF localizes mainly to the ER at steady state. Post-nuclear membranes from yeast cells were separated on isopycnic sucrose gradients in the presence of Mg^{2+} or EDTA. Proteins were detected by SDS–PAGE and immunoblotting of the fractions. Correctly inserted FT-FF cofractionates with Sec63, an ER transmembrane protein, but away from Gda1, a Golgi transmembrane protein, and Pma1, a plasma membrane transmembrane protein.

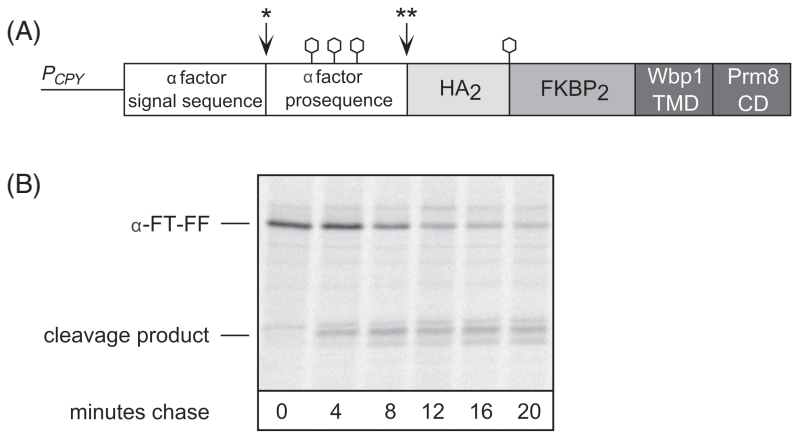

Figure 2: α-FT-FF travels through the secretory pathway in live cells. A) Design of the α-FT-FF construct. Line, promoter region; box, protein coding region. The CPY signal sequence is replaced by the signal sequence and the prosequence of yeast α-factor resulting in the protein α-FT-FF. The single asterisk indicates cleavage of the protein by signal peptidase in the ER. The double asterisk indicates cleavage of the protein by Kex2 in the trans-Golgi. Each hexagon depicts a glycosylation site in the protein. B) The α-FT-FF construct travels to the Golgi apparatus. After a radioactive 3-min pulse and the indicated chase times, cells were lysed and proteins were precipitated with anti-HA antibody. The position of the full-length protein (following signal sequence cleavage) and the Kex2 cleavage product are indicated.

of the lumenally oriented, upper band FT-FF protein in the absence of detergent can also be seen for the control protein Kar2, a lumenal ER chaperone, indicating a partial permeability of the microsomes for proteinase K. The *N*-ethylmaleimide-sensitive-factor attachment receptor (SNARE) protein Sec22 was only partially sensitive for this protease, even if applied in higher concentrations (data not shown). Taken together, our data support a dual membrane topology for FT-FF as reported for several prokaryotic and eukaryotic proteins. Dual membrane topology is determined by amino acid sequence as well as by membrane lipid composition (50–53).

To establish the intracellular localization of FT-FF, we separated membranes from a glass bead homogenate of yeast cells on isopycnic sucrose gradients in the presence and absence of magnesium. Between these two conditions, ER membranes undergo a characteristic density shift owing to the dissociation of the ribosomes at low magnesium concentrations (54). Both bands of the FT-FF doublet fractionated together with the ER membrane marker Sec63 but away from the plasma membrane protein Pma1 and the Golgi marker Gda1 (GDPase; Figure 1E). Thus, at steady state FT-FF is mainly localized to the ER, suggesting that the monomeric protein either fails to exit the ER or is efficiently retrieved from a post-ER compartment.

To test whether our FKBP fusion protein could exit the ER in living cells, we replaced the signal sequence of CPY with the signal sequence and the prosequence of yeast alpha-factor (α-factor), which contains a dominant export signal that binds to the Erv29 cargo receptor (55,56) (Figure 2A). Because the α-factor prosequence is cleaved by the Kex2 protease in the trans-Golgi region (57), the progress of the fusion proteins through the cell can be easily monitored. We found in a pulse-chase experiment that the resulting protein, termed α-FT-FF, was transported from the ER to the trans-Golgi region *in vivo* (Figure 2B); thus, the core domains of the construct apparently do not contain dominant retention signals that inhibit ER export. The α-FT-FF protein appeared as a single band, suggesting that it was inserted into the membrane in type I orientation only.

We next induced oligomerization of FT-FF. Addition of AP20187 to *Saccharomyces cerevisiae* cultures did not lead to oligomerization of FT-FF (data not shown), probably because of inefficient uptake of the drug or export from the cells by a pleiotropic drug resistance pump (58). Therefore, we used an *in vitro* system. To this end, we prepared

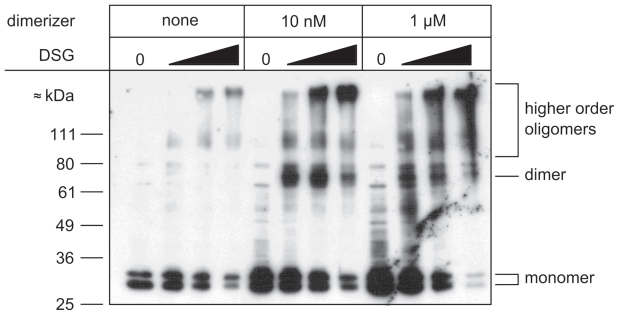

Figure 3: FT-FF forms oligomers upon addition of the dimerizer, AP20187. Microsomes were incubated with dimerizer at the indicated concentrations and proteins were then cross-linked with increasing concentrations (0, 100, 200 and 400 μM) of the non-cleavable cross-linker, DSG, separated by SDS–PAGE and detected by immunoblotting.

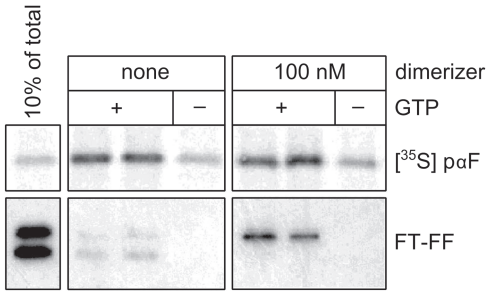

Figure 4: Packaging of FT-FF into COPII vesicles *in vitro* depends on the concentration of dimerizer and is specific for the glycosylated form of the protein. Microsomes were incubated with dimerizer at the indicated concentrations and with COPII components in the presence or absence of bud-inducing GTP as indicated. COPII vesicles were then separated from the donor membranes by centrifugation, and proteins recovered from the vesicular supernatant were separated by SDS–PAGE. FT-FF was detected by immunoblotting, and [^{35}S] pαF, radioactive pro-α factor, by phosphoimaging.

microsomal membranes from yeast cells that expressed the gene fusion and added increasing concentrations of AP20187 dimerizer. After incubation at 10°C for 30 min, we added the irreversible amino-reactive cross-linker disuccinimidyl glutarate (DSG). Analysis of the reaction products by SDS–PAGE and immunoblotting showed a specific crosslink, corresponding in size to a dimer of the fusion protein, which occurs only in samples treated with both dimerizer and DSG (Figure 3). Under these conditions, cross-linked oligomers of higher molecular weight were also detected. At a dimerizer concentration of 1 μM, more FT-FF monomers (both upper and lower species) were consumed by cross-linking, but the dimer band appeared less prominent compared to 10 nM dimerizer because higher order oligomers became more apparent. We conclude that the dimerizer induces FT-FF to form oligomers in microsomal membranes *in vitro*, and that the FKBP domains of the fusion protein are functional.

An oligomeric form of FT-FF is preferentially packaged into COPII vesicles

To test whether oligomerization of FT-FF influenced its packaging into COPII vesicles, we performed *in vitro* COPII budding assays (1) with isolated microsomal membranes or radiolabeled semi-intact cells and assessed the packaging of the fusion protein. In the absence of the dimerizer, only low levels of FT-FF were packaged into vesicles with no significant preference for the upper or lower band species. When dimerizer was added to the budding reaction, the upper (putatively type I-oriented, glycosylated, trypsin-resistant) but not the lower (type II-oriented, unglycosylated, trypsin-sensitive) band was found enriched in the COPII vesicle fraction (Figure 4, lower panel). As controls, we examined the packaging of the soluble secretory protein pro-α factor (Figure 4, upper panel) and the vacuolar membrane protein Vph1 (see below) and found that dimerizer had no effect. Thus, oligomerization of the type I-inserted fusion protein strongly increased its recruitment into COPII vesicles.

The diphenylalanine in the cytosolic tail of FT-FF binds to Sec23/24

We next investigated the molecular mechanism for the preferred packaging of oligomers. Initially, we hypothesized that upon oligomerization, an avidity effect might stabilize the weak interactions between the cytosolic tail of FT-FF and the COPII coat. On the basis of this assumption, we postulated that altering the sequence of the cytosolic tail to decrease its COPII-binding affinity should reduce or abolish its packaging into COPII vesicles and the oligomerization effect.

To test this hypothesis, we set out to find a variant of the cytosolic tail of Prm8 that bound less tightly

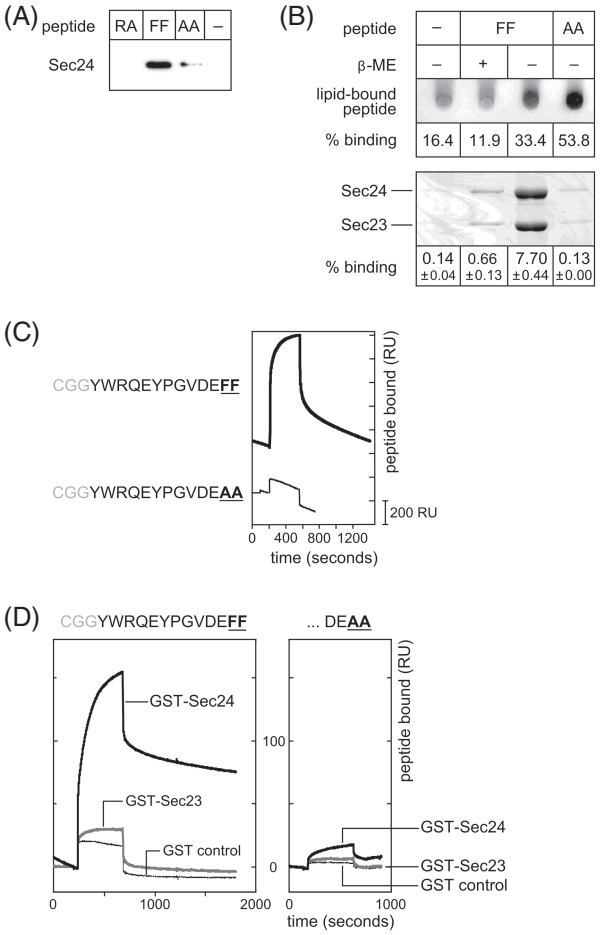

Figure 5: Legend on opposite side.

to COPII proteins, and we changed the C-terminal diphenylalanine motif in the wild-type tail sequence (13,25), YWRQEYPGVDEFF (Prm8-FF). We found that agarose beads modified with a peptide corresponding to the Prm8-FF tail sequence bound the Sec24 protein from yeast cytosol. In contrast, replacement of the C-terminal phenylalanines with alanines (Prm8-AA peptide) resulted in much diminished binding, whereas use of a randomized sequence peptide, or no peptide, gave no Sec24 binding (Figure 5A). Similarly, recombinant Sec23/24 complex bound to liposomes modified with the Prm8-FF peptide, but not the Prm8-AA peptide, demonstrating that binding is direct and can occur on a lipid surface (Figure 5B). We next attached recombinant Sec23/24 complex or the individual Sec23 and Sec24 proteins onto a surface plasmon resonance (SPR) sensor chip and added the Prm8 tail peptides to the flow of buffer across the sensor surface. The Prm8-FF peptide bound significantly better than the Prm8-AA peptide to Sec23/24 and Sec24, but to Sec23, no binding was observed (Figure 5C, D). We conclude that the binding of the Prm8 cytosolic tail to Sec24 requires the FF motif.

In vitro COPII budding of type I-inserted FT constructs is enhanced by oligomerization independently of COPII-binding motifs

We next explored the correlation between Sec23/24-binding activity and packaging into COPII vesicles.

Figure 5: The cytosolic Prm8 peptide interacts directly with Sec24. A) Sec24 binds to the Prm8-FF peptide. Sec23/24 pull-down assay using agarose beads derivatized with peptides (FF, wild-type Prm8-FF peptide; AA, Prm8(FF → AA) peptide; RA, randomized peptide). Beads were incubated with yeast cytosol, and Sec24 was detected in the bead-bound fraction by SDS–PAGE and immunoblotting. B) Sec24 binding to Prm8-FF peptide is direct. Sec23/24 binding to liposomes carrying the Prm8 peptide. Peptides (FF and AA as above) were reacted with liposomes containing maleimide-derivatized lipids. The extent of peptide–lipid coupling was estimated from the lipid material that remained at the origin of a TLC plate (upper panel, and quantification). Peptide-conjugated liposomes were incubated with Sec23/24 and floated through an iodixanol gradient to remove unbound protein. Membrane-bound Sec23/24 was detected by SDS–PAGE and SYPRO Red staining (lower panel). Sec23 and Sec24 recovery was quantified independently and averaged. The error is the standard deviation of the individual values from the average. C) Prm8-FF but not Prm8-AA peptide binds to Sec23/24. Purified Sec23/24 complex was non-covalently attached to the surface of a SPR sensor through the His_6 tag on Sec24. To assess binding, we added the indicated peptides at 80 μM to the flow of buffer across the sensor, and RUs were recorded. Background signals (from a protein-free flow cell) were subtracted. A constant downward slope is visible in all curves owing to the slow dissociation of the Sec23/24 complex from the sensor chip. D) The Prm8-FF peptide binds to Sec24 but not to Sec23. GST (thin line), GST-Sec23 (gray line) and GST-Sec24 (thick black line) were bound to sensor surfaces covalently modified with anti-GST antibody, and dimeric peptides were added to the flow of buffer across the sensor. Background signals (from a flow cell containing only antibody) were subtracted.

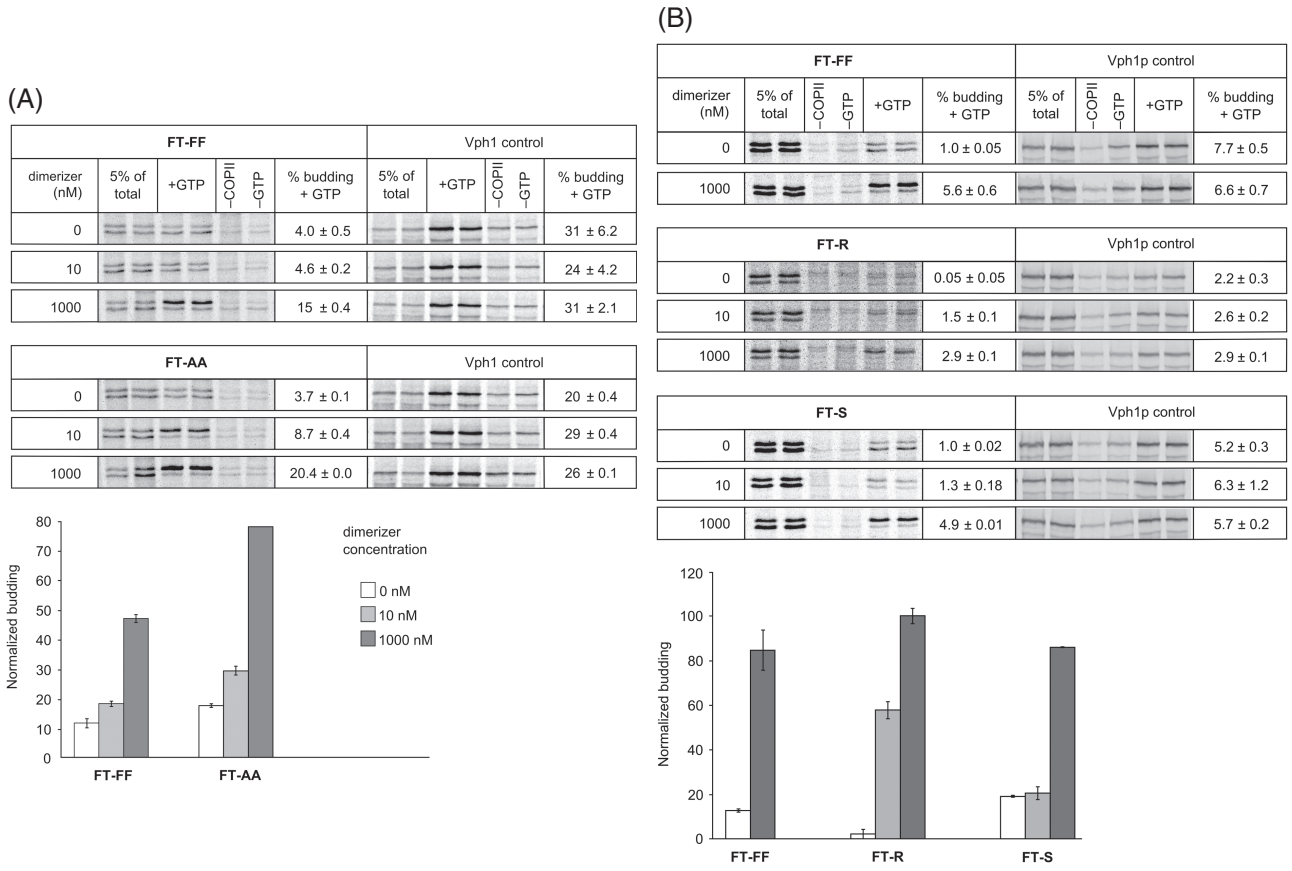

Figure 6: The cytosolic tail of FT constructs has no influence on their *in vitro* COPII packaging. A) FT-FF and FT-AA are packaged into COPII vesicles with similar efficiency. Proteins were precipitated from vesicular supernatants of budding reactions that had been performed using radiolabeled semi-intact cells in the presence of the indicated concentrations of dimerizer. Budding percentages are given for the FKBP fusions (upper band) and for Vph1 as budding control. Errors are the standard deviation of duplicates. The bar charts show packaging of the constructs (upper band) normalized against the control protein Vph1. B) FT-FF, FT-R and FT-S are packaged into COPII vesicles with similar efficiency. This experiment was performed as in (A) with the exception that semi-intact cells were washed more stringently with high-salt buffer before the budding reaction to remove all endogenous-bound COPII proteins. As a result, the overall budding rates were lower (compare the values for FT-FF in panels A and B).

To this end, we constructed the fusion protein FT-AA, which is identical to FT-FF, except that the C-terminal phenylalanines are replaced with alanines. Given that in all four independent experiments, the Prm8-AA peptide showed some (though greatly reduced) binding to Sec23/24, we also constructed two other fusion proteins that, instead of cytosolic tails, had just a single amino acid following the transmembrane domain (arginine: FT-R or serine: FT-S). When expressed in yeast, these fusion proteins displayed the same membrane localization as well as trypsin and EndoH sensitivity as we observed for FT-FF (data not shown).

We then performed *in vitro* COPII budding experiments with all four fusion proteins in the presence and absence of the dimerizer, focusing our analysis on the upper band type I-inserted protein, in which C-terminal-binding motifs are directed toward the cytosol. Interestingly, both FT-FF and FT-AA showed a fourfold to fivefold increase in budding efficiency when 1 μM dimerizer was present, while packaging of the control protein Vph1 (YOR270C), a vacuolar ATPase subunit that is well exported from the ER, was not influenced by dimerizer (Figure 6A). Similar levels of dimerizer-stimulated packaging into COPII vesicles were observed with FT-R and FT-S (Figure 6B). Thus,

the difference in COPII-binding affinity of the cytosolic domains appears to be irrelevant for uptake of these proteins into COPII vesicles *in vitro*, and we conclude that dimerizer-stimulated packaging of our model protein into COPII vesicles is not caused by an avidity effect in binding to Sec24.

Discussion

We have constructed a chimeric, oligomerization-competent membrane protein, FKBP-TMD-FF (FT-FF), to investigate the influence of cargo protein oligomerization on ER export. The cytosolic tail of the construct contains two distinct sequence motifs that have been implicated in promoting transport of membrane proteins out of the ER, neither of which significantly contributed to the packaging of the fusion protein into COPII vesicles. The C-terminal diphenylalanine (FF) motif is also present in the cytosolic tail of some p24 proteins (13,59) and of ERGIC-53, where mutation leads to a decreased ER export of the protein *in vivo*, concurrent with diminished *in vitro* binding to COPII proteins (14,25).

We have established by three independent techniques that binding of Sec24 to the Prm8-derived cytosolic tail sequence of FT-FF indeed depends on the C-terminal phenylalanines. Still, FT-FF and FT-AA are packaged into COPII vesicles with the same efficiency *in vitro*, and addition of dimerizer dramatically enhances packaging of both fusion proteins (Figures 4 and 6). Another potential export motif identified in some proteins, F/Yx$_4$F/Y (13,45), is present in the Prm8 sequence: CGGYWRQEYPGVDEFF. We have not conducted binding experiments in which this sequence was modified, but because FT-R and FT-S both showed dimerizer-dependent budding to the same extent as FT-FF (Figure 6B), we assume that this sequence does not mediate the degree of packaging into COPII vesicles in our system.

The hypothesis that oligomerization signifies the culmination of protein synthesis and folding in the ER, and simultaneously a signal to initiate export, was formulated some time ago (22,37,60,61). Numerous examples of proteins that might act in this way have been documented, such as the T-cell receptor (62), influenza virus hemagglutinin (a homotrimer) (63), ERGIC-53 (a homohexamer) (64,65), vesicular stomatitis virus G protein (a homotrimer) (64,66), sodium-dependent neurotransmitter transporters (67), the yeast Vig4/Gog5p transporter (a homodimer) (68,69) as well as yeast Erv41p/Erv46p (70) and Emp46p/Emp47p heterodimers (38). Similarly, the *N*-acetylglucosamine-1-phosphotransferase (PT) α/β-subunit precursor protein can be transported only if a combinatorial sorting motif forms an epitope in the heterodimer, which can be recognized by the COPII machinery, suggesting that oligomerization can generate export motifs missing in the single subunits (71) thereby indicating the completion of protein folding. Our findings now provide a confirmation of this hypothesis for a model protein and constitute a novel example for a protein without a known (or indeed possible) cytosolic export signal.

We first assumed that formation of oligomers would lead to the presentation of the C-terminal cytosolic tails to the COPII coat as a linked oligomeric array and thus increase the avidity of the interaction between coat and cargo proteins as shown for the γ-aminobutyric acid (GABA) transporter 1 (GAT 1) (72,73). However, our results provide evidence for a novel effect of oligomerization as the cytosolic tail of the fusion protein seems to have no influence on the efficiency of export from the ER membranes: both COPII-binding and non- (i.e. weak-) COPII-binding constructs (FT-AA, Figure 5; FT-R, -S; data not shown) show dimerizer-dependent ER exit (Figure 6A, B). Our data thus support the hypothesis that the oligomeric state of a membrane protein itself can act as an ER export signal without the need to bind to the cytosolic COPII components. The possibility remains that oligomers interact with a cargo receptor via the transmembrane or lumenal domains that would serve as a link to the COPII coat, but we have no reason to believe that either the HA epitope tags or the FKBP domains would have such a cargo receptor in yeast.

Another mechanism that deserves consideration involves dominant retention. In some cases, formation of hetero-oligomers masks retrieval and/or retention signals on subunits in a complex and thus moves the steady-state location of a protein to the Golgi apparatus and beyond: the chloride channel Kir6.2 (74) and connexin-43 contain cytosolic arginine motifs that are masked (75), the IgE receptor (76) and the lipid phosphatase Sac1 contain

dilysine motifs that are masked (77), the T-cell receptor has charged residues in its transmembrane domains that must be properly paired (61,78) and the asialoglycoprotein receptor subunits are retained by ER lumenal pentapeptide sequences unless they are joined together in the dimer (79). We believe that this does not occur with the FKBP constructs because the α-FT-FF fusion protein is transported rapidly and efficiently out of the ER *in vivo*, suggesting that there is no dominant retention signal on the FKBP or TMD sequences (Figure 2B). Moreover, we do not observe major cross-links of FT-FF to any other protein in the absence of dimerizer (Figure 5). We cannot, however, exclude that interaction of the prosequence with the cargo receptor Erv29 could outbalance retentive chaperone binding *in vivo*.

Another explanation for our observations is that oligomerization of our model protein changes its physical properties such that it becomes enriched in COPII budding sites, for example, in regions of curved membrane or in regions of different lipid composition (80–82). This mechanism is known to act in other steps in vesicular trafficking where oligomerization-induced transport has been demonstrated. For instance, the binding of antigen by the B-cell receptor at the cell surface leads to its oligomerization in lipid rafts (probably brought about by the altered physical properties of the oligomer) and internalization (83), and a similar mechanism is postulated for the Fcε receptor (84). In early endosomes, targeting of Fc and transferrin receptors toward lysosomes is enhanced by oligomerization (85); a lipid-based sorting mechanism may be at work here, too (86). Furthermore, it is well known that proteins and protein complexes can force lipid membranes to bend, e.g. rigid proteins exhibiting domains of intrinsic curvature like the banana-shaped Bin-Amphiphysin-Rvs (BAR) domain, or the COPII coat protein complexes Sec23/24 and Sec13/31, which have a concave membrane contact surface after polymerization (87–89). Copic et al. have recently shown that Sec13 is dispensable for the generation of COPII vesicles when non-essential membrane cargo proteins are depleted, proposing that asymmetrical membrane cargo (e.g. glycosyl-phosphatidylinositol-anchored or p24-family proteins with their mass at the luminal side of the ER membrane) might cause an inward, concave curvature of the membrane (into the ER lumen) (90). This inward curvature resisted the formation of convex COPII buds and could only be overcome by a fully functional COPII coat, rigid enough to enforce a concave, outward curvature and thus the generation of a transport vesicle (90,91). The antagonism between membrane curving protein coats that drive vesicle formation and energy barriers (generated for instance by lumenally oriented membrane proteins) that oppose it were recently reviewed by Stachowiak et al. (92).

Intriguingly, for our FT fusion proteins we observed that packaging of the lower band species (which we believe are inserted into the membrane in a type II orientation) into COPII vesicles often became less efficient as the concentration of dimerizer was increased (this is especially well visible for FT-FF in Figure 4 and for FT-S in Figure 6B). This suggests that a membrane curvature model provides the simplest explanation for the oligomerization-induced enhancement of COPII packaging that we observe. We hypothesize that the lower mobility FT species, correctly inserted in the type I orientation, forms an oligomer that fits better into or even supports formation of the convex COPII buds (Figure 7). In contrast, the higher mobility type II-oriented oligomer may locally impart a concave shape on the ER membrane that is not conducive to COPII vesicle formation and this form is therefore excluded from COPII vesicles.

Whichever mechanism causes the increased packaging of oligomeric proteins, it is tempting to envisage situations in which the degree of oligomerization of a protein is used to control its export from the ER *in vivo*. First, correct folding and maturation of a protein are required for oligomerization (see above), ensuring that only correctly folded proteins enter the secretory pathway. Second, membrane protein oligomerization in the ER can be induced by the binding of a ligand to the lumenal domain, in analogy to the ligand-induced dimerization of cell surface receptors. In this manner, lumenal cargo proteins could bind to their transmembrane receptors via protein or glycan residues, bring about their oligomerization and COPII binding and thus initiate their own uptake into ER to Golgi transport vesicles. Such a mechanism has been described in the Golgi apparatus for the induction of COPI vesicle formation by the KDEL receptor, Erd2 (93). Third, a conformational change in a protein could lead to an increase in affinity for a specific domain of the

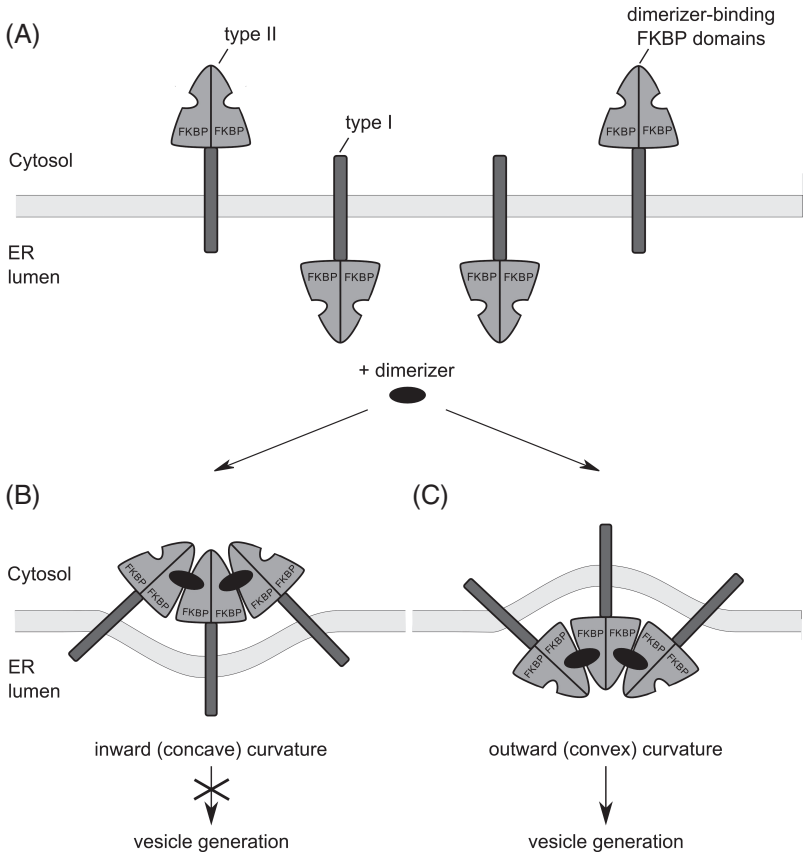

Figure 7: One hypothetic model: FT-FF influences membrane bending upon dimerization. A) FT-FF is randomly inserted into the ER membrane in type I and type II orientation (lower and faster mobility species in the gels, respectively, see, e.g. Figure 5). B and C) Addition of the dimerizer AP20187 results in polymerization of the respective FT-FF species. We hypothesize a complex conformation that strongly imparts membrane bending (depicted as triangular FKBP domains): The type II-oriented oligomer favors a concave membrane curvature opposing vesicle generation (B), whereas the type I-oriented oligomer induces convex membrane bending thereby facilitating COPII vesicle formation (C). HA_2 tag and glycans of the protein construct are omitted for clarity.

ER membrane (e.g. a lipid raft), which may then lead to its oligomerization owing to its increased concentration in such a domain.

Materials and Methods

Peptide-binding assays

Peptides were prepared, high-performance liquid chromatography-purified to homogeneity and the sequence was confirmed by mass spectroscopy by David King (HHMI and UC Berkeley, CA, USA) and the HHMI/Keck Facility (Yale University, CT, USA). For peptide-binding experiments, 2.5 mg of peptides [Prm8 = CGGYWRQEYPGVDEFF, Prm8(FF → AA) = CGGYWRQEYPGVDEAA, randomized sequence = CGGFPFYEEQGVWRDY] was coupled to 500 µL Sulfo-Link agarose (Thermo Scientific) in the presence of 50 mM Tris–Cl pH 8.5, 5 mM ethylenediaminetetraacetic acid (EDTA) and 50 mM TCEP [Tris(2-carboxyethyl)phosphine hydrochloride] according to the manufacturer's instructions. For peptide binding, 20 µL of beads was washed with BB2 [20 mM K-HEPES, pH 6.8, 160 mM potassium acetate, 5 mM magnesium acetate, 2% (v/v) glycerol, 1 mM DTT, 1 mM EDTA and 0.2% octyl glucoside] and incubated with 180 µL of BB2 and 20 µL of cytosol (protein content 10 mg/mL; preparation described in 94) for 2 h at 4°C. The beads were washed twice with BB2 and once with 20 mM Tris–Cl, pH 7.0, 150 mM NaCl, and proteins were resolved by SDS–PAGE and detected by immunoblotting.

Liposomes were prepared essentially according to 95. The lipid mixture (all from Avanti Polar Lipids) was 20% (w/w) ergosterol and 80% (w/w) phospholipids, with a phospholipid composition of 77 mol% dioleoylphosphatidylcholine (DOPC), 8 mol% dioleoylphosphatidylethanolamine (DOPE), 8 mol% 1-palmitoyl-2-oleoyl-phosphatidylethanolamine (POPE), 2 mol% dioleoyl-[*N*-(7-nitrobenz-2-oxa-1,3-diazoyl-4yl)]-*sn*-glycero-phosphoethanolamine (NBD-PE) and 5 mol% *N*-[4-(*p*-maleimidophenyl)-butyramido]-1,2-dioleoyl-*sn*-glycero-phosphoethanolamine (N-MPB-PE). Lipids were mixed, dried, hydrated in 20 mM K-HEPES, pH 6.0, with 270 mM sucrose and extruded through a 400-nm filter. Liposomes were then sedimented for 15 min at 245 000 × ***g*** and resuspended in HK6.7 (20 mM HEPES, pH 6.7 and 160 mM KOAc) to a lipid concentration of 2 mM. Peptide solutions (750 µM) were supplemented with 4 mM TCEP, incubated for 10 min and added to an equal volume of liposome suspension. Coupling was carried out at room temperature for 90 min, and was terminated by addition of beta-mercaptoethanol (β-ME) to 8 mM. In some controls, β-ME was added prior to the peptide. The liposomes were sedimented as above and washed with HK7.0 to remove free peptides. Peptide–phospholipid coupling was analyzed by thin layer chromatography (TLC) on silica gel plates (Whatman HPK60A), which were developed with chloroform:methanol:acetate (13:7:1), stained

with 0.005% primulin in water:acetic acid (1:4) and read in the blue fluorescence channel of a STORM image analyzer (GE Healthcare Life Sciences). The signal for peptide-coupled MPB-PE (retarded at the origin) was quantified, corrected for plate background and expressed as a percentage of the DOPC signal in the same lane.

Binding of Sec23/24 to liposomes was assessed essentially according to 95 with the following alterations: Binding reactions (75 μL total volume) were adjusted to 125 μL with 23% (w/v) iodixanol (OptiPrep, Nycomed), and 100 μL of this solution was overlaid with 75 μL 18% (w/v) iodixanol in HK7.0 and 25 μL HK7.0 in 7′11-mm polycarbonate tubes. This gradient was centrifuged for 20 min at 436 000× ***g*** (2°C), and the top 50 μL was withdrawn. Lipid recovery was assessed by NBD-PE fluorescence in microtiter plates using a STORM image analyzer. Sec23/24 was quantified by SDS–PAGE (sample loading normalized for lipid recovery), SYPRO Red staining and STORM image analysis.

For the SPR (Biacore, GE Healthcare Life Sciences) experiments, the manufacturer's instructions and reagents were used to immobilize proteins to sensor surfaces. For Figure 4C, 11 000 resonance units (RUs) of Sec23/24 were immobilized on an NTA sensor chip via the C-terminal His_6 tag of Sec24, and peptide binding was performed in BB4 (300 mM potassium acetate, 20 mM K-HEPES, pH 6.8 and 0.01% TX-100) at 80 μM peptide, various concentrations of β-ME, 4 μL/min and 10°C. For Figure 4D, GST, GST-Sec23 and GST-Sec24 were prepared from *Escherichia coli* as published (96). Anti-GST antibody (4800–6200 RU) and about 1000 RU of GST, 1100 RU of GST-Sec23 and 1400 RU of GST-Sec24 were immobilized to a CM5 surface, and peptide binding was performed in BB4 at 80 μM peptide, 5 μL/min flow and 20°C.

Cloning of FT constructs

To construct the *FT-FF* gene, we ligated the EcoRI–BamHI fragment of pCYI-20 (43) containing the CPY promoter and signal sequence into EcoRI/BamHI cut pRS316 (*URA3 CEN*) (97). To insert two HA tags and a glycosylation site, we cut the resulting plasmid with BamHI and XbaI and the oligonucleotides oSP71 (5′-GAT CCG TAT CCA TAT GAT GTT CCA GAT TAT GCT TAC CCT TAC GAC GTA CCT GAC TAC GCA GCA AAT TCT ACT AGA TCT ACT AGT T) and oSP72 (5′-CTA GAA CTA GTA GAT CTA GTA GAA TTT GCT GCG TAG TCA GGT ACG TCG TAA GGG TAA GCA TAA TCT GGA ACA TCA TAT GGA TAC G) were annealed and ligated into the gap to yield pSP51. That plasmid was cut with SpeI and an XbaI-SpeI fragment from $pC_4M\text{-}F_v2E$ (Ariad Pharmaceuticals) containing two FKBP(F36V) domains in tandem was inserted to obtain pSP52. To add the Wbp1 transmembrane domain, oligos oSP472-1 (5′-CTA GCG AAA TTT CTA ACT CTT GGG TTT ACA TTT CTG CTA TTT GTG GTG TTA TTG TTG CTT GGA TTT TCT TCG TTG TTT CTT TCG TTA CTA CTT CTT CTG TTG GTA) and oSP472-2 (5′-CTA GTA CCA ACA GAA GAA GTA GTA ACG AAA GAA ACA ACG AAG AAA ATC CAA GCA ACA ATA ACA CCA CAA ATA GCA GAA ATG TAA ACC CAA GAG TTA GAA ATT TCG) were annealed and ligated into the SpeI site of pSP52, giving pSP75. To obtain the *CEN* expression vector for FT-FF, pSP77, pSP75 was cleaved with SpeI and SacI, and the oligos oSP472-3 (5′-CTA GTT ACT GGA GAC AAG AAT ACC CAG GTG TTG ATG AAT TCT TCT AAG AGC T) and oSP472-4 (5′-AAT GAC CTC TGT TCT TAT GGG TCC ACA ACT ACT TAA GAA GAT TC) were annealed and inserted. The *CEN* expression vector for FT-AA, pSP79, was generated in an analogous manner using the oSP472-5 (5′-CTA GTT ACT GGA GAC AAG AAT ACC CAG GTG TTG ATG AAG CTG CTT AAG AGC T) and oSP472-6 (5′-AAT GAC CTC TGT TCT TAT GGG TCC ACA ACT ACT TCG ACG AAT TC) oligos. The corresponding 2μ vectors, pSP81 and pSP83, were made from pSP77 and pSP79 by transferring the *Hin*dIII-SacI fragments to pRS425 (97). All cloning operations were confirmed by sequencing. To generate α-FT-FF, we isolated the DNA sequence encoding the α-factor leader and prosequence from pSEY210 (98) by digestion with EcoRI and *Hin*dIII, filled in with Klenow polymerase and ligated into the filled-in backbones of pSP81 and pSP83 isolated after *Hin*dIII/BamHI digestion to give pSP86 and pSP87.

Characterization of FT-FF

For protein extraction experiments, we suspended logarithmically growing cells in STM10 (54) and lysed with glass beads. The crude lysate was centrifuged for 5 min at 500× ***g***, and the supernatant was transferred to a new tube and centrifuged at 13 000× ***g*** for 15 min. The pellet was resuspended in STM10, Triton buffer (1% Triton X-100 in 150 mM NaCl, 10 mM Tris–Cl, pH 7.5), 100 mM Na_2CO_3 or in 2.5 M urea in 10 mM Tris–Cl, pH 7.5, and rotated at 4°C for 1 h. The suspension was centrifuged at 100 000× ***g*** for 1 h. Proteins were recovered from pellets (resuspended in Triton buffer) and supernatants by methanol/chloroform precipitation (99), separated by SDS–PAGE and detected by immunoblotting. For the EndoH digestion, we labeled cells and proteins extracted from lysates were precipitated and digested as described (44) with small alterations: labeling was with 5.5 μL (2.9 MBq) of 35S Promix (GE Healthcare Life Sciences) for 2.2 OD equivalents of cells, the chase was omitted and preclearing was with 50 μL of IgSorb suspension (The Enzyme Center). For the protease digestion, we incubated microsomes containing 18 μg of total protein in 40 μL B88 with 5 μg/mL proteinase K (Sigma Aldrich) for 5 min on ice. Where indicated, Triton X-100 was added to a final concentration of 1%. The reactions were quenched with 10 mM phenylmethylsulfonylfluoride and proteins were precipitated using trichloroacetic acid at a final concentration of 15%. After a centrifugation at 20 000× ***g*** for 15 min at 4°C, pellets were washed in 500 μL of chilled acetone and resuspended in 20 μL SDS sample buffer. Samples were heated to 55°C for 10 min, separated by SDS–PAGE and detected by immunoblotting. Isopycnic sucrose gradient centrifugations were performed as described (54), with the alteration that the 12 mL gradients (20–60% sucrose) were fractionated at 700 μL per fraction, giving 18 fractions. Proteins were recovered by methanol/chloroform precipitation and detected by SDS–PAGE and immunoblotting. For the cross-linking experiment, we incubated yeast microsomes corresponding to 128 μg of protein in B88 containing ATP mix and dimerizer (from a 100× stock in EtOH) in a total volume of 100 μL for 30 min at 10°C. The membranes were sedimented by centrifugation for 5 min at 12 500× ***g*** and washed twice with and resuspended in B88 containing dimerizer. Samples were split into four and aliquots were incubated with increasing amounts (0, 100, 200 and 400 μM) of DSG (from a 10× stock in DMSO)

for 20 min at 20°C. To quench the cross-linker, we added ammonium acetate to 400 mM, and the incubation was continued for 10 min on ice. The proteins in the sample were then separated by SDS–PAGE and detected by immunoblotting. Microsome isolation, B88 and 10× ATP mix are described in 94.

In vitro vesicle generation (budding) and *in vivo* pulse-chase experiments

COPII component proteins were purified, microsomal membranes from yeast were isolated and COPII *in vitro* budding reactions were conducted as described (94). For the experiments shown in Figures 4 and 6, we included dimerizer throughout the budding reactions. COPII protein concentrations in the budding reactions were 20 μg/mL for Sar1, 20 μg/mL for Sec23/24 and 40 μg/mL for Sec13/31. Proteins were recovered from the medium-speed supernatant by methanol/chloroform precipitation, separated by SDS–PAGE and detected by immunoblotting (for FT-FF or FT-AA) or quantitative phosphoimaging (for pro-α factor).

The pulse-chase experiment with immunoprecipitation was carried out essentially as described (44) with the following alterations: 40 min prior to labeling, cells were transferred into prestarving medium (minimal medium minus leucine, methionine, cysteine and with homoserine instead of threonine; Qbiogene). Pulse labeling was for 5 min. Preclearing was with 30 μL IgSorb. Immunoprecipitation was with 3 μg affinity-purified anti-HA monoclonal antibody (Covance). Immunoprecipitated proteins were separated by SDS–PAGE and detected using a STORM phosphoimager.

Acknowledgments

Our special thanks go to Robert Lesch for repeating the protease protection assay. We further thank Ira Mellman and Jim Miller for discussions; Susanne Fritzsche, Sharif Ahmed, Art Johnson, Marcus Lee, David Madden and Elizabeth Miller for improving the manuscript; Ariad for supplying the dimerizer reagent and the FKBP plasmids; Alison Watta (Biacore, GE Healthcare Life Sciences) for help and reagents; Robert Lesch and Crystal Chan for COPII protein preparations; and David King for peptides. S. S. was supported as an HHMI (Howard Hughes Medical Institute) Research Associate. R. D. was supported by the DFG Excellence Cluster 'Inflammation at Interfaces'. R. S. is an investigator of the Howard Hughes Medical Institute and a Senior Fellow of the Miller Institute at the University of California in Berkeley.

References

1. Barlowe C, Orci L, Yeung T, Hosobuchi M, Hamamoto S, Salama N, Rexach MF, Ravazzola M, Amherdt M, Schekman R. COPII: a membrane coat formed by Sec proteins that drive vesicle budding from the endoplasmic reticulum. Cell 1994;77:895–907.
2. Lee MC, Miller EA. Molecular mechanisms of COPII vesicle formation. Semin Cell Dev Biol 2007;18:424–434.
3. Hughes H, Stephens DJ. Assembly, organization, and function of the COPII coat. Histochem Cell Biol 2008;129:129–151.
4. Lederkremer GZ, Cheng Y, Petre BM, Vogan E, Springer S, Schekman R, Walz T, Kirchhausen T. Structure of the Sec23p/24p and Sec13p/31p complexes of COPII. Proc Natl Acad Sci U S A 2001;98:10704–10709.
5. Matsuoka K, Schekman R, Orci L, Heuser JE. Surface structure of the COPII-coated vesicle. Proc Natl Acad Sci U S A 2001;98:13705–13709.
6. Gillon AD, Latham CF, Miller EA. Vesicle-mediated ER export of proteins and lipids. Biochim Biophys Acta 2012;1821:1040–1049.
7. D'Arcangelo JG, Stahmer KR, Miller EA. Vesicle-mediated export from the ER: COPII coat function and regulation, Volume 1833. Biochim Biophys Acta: ; 2013, pp. 2464–2472.
8. Wieland FT, Gleason ML, Serafini TA, Rothman JE. The rate of bulk flow from the endoplasmic reticulum to the cell surface. Cell 1987;50:289–300.
9. Thor F, Gautschi M, Geiger R, Helenius A. Bulk flow revisited: transport of a soluble protein in the secretory pathway. Traffic 2009;10:1819–1830.
10. Klumperman J, Schweizer A, Clausen H, Tang BL, Hong W, Oorschot V, Hauri HP. The recycling pathway of protein ERGIC-53 and dynamics of the ER-Golgi intermediate compartment. J Cell Sci 1998;111:3411–3425.
11. Balch WE, McCaffery JM, Plutner H, Farquhar MG. Vesicular stomatitis virus glycoprotein is sorted and concentrated during export from the endoplasmic reticulum. Cell 1994;76:841–852.
12. Malkus P, Jiang F, Schekman R. Concentrative sorting of secretory cargo proteins into COPII-coated vesicles. J Cell Biol 2002;159:915–921.
13. Dominguez M, Dejgaard K, Füllekrug J, Dahan S, Fazel A, Paccaud JP, Thomas DY, Bergeron JJ, Nilsson T. gp25L/emp24/p24 protein family members of the cis-Golgi network bind both COP I and II coatomer. J Cell Biol 1998;140:751–765.
14. Nufer O, Guldbrandsen S, Degen M, Kappeler F, Paccaud JP, Tani K, Hauri HP. Role of cytoplasmic C-terminal amino acids of membrane proteins in ER export. J Cell Sci 2002;115:619–628.
15. Dancourt J, Barlowe C. Protein sorting receptors in the early secretory pathway. Annu Rev Biochem 2010;79:777–802.
16. Saito K, Chen M, Bard F, Chen S, Zhou H, Woodley D, Polischuk R, Schekman R, Malhotra V. TANGO1 facilitates cargo loading at endoplasmic reticulum exit sites. Cell 2009;136:891–902.
17. Malhotra V, Erlmann P. Protein export at the ER: loading big collagens into COPII carriers. EMBO J 2011;30:3475–3480.
18. Venditti R, Scanu T, Santoro M, Di Tullio G, Spaar A, Gaibisso R, Beznoussenko GV, Mironov AA, Mironov A Jr, Zelante L, Piemontese MR, Notarangelo A, Malhotra V, Vertel BM, Wilson C, et al. Sedlin controls the ER export of procollagen by regulating the Sar1 cycle. Science 2012;337:1668–1672.
19. Lord C, Ferro-Novick S, Miller EA. The highly conserved COPII coat complex sorts cargo from the endoplasmic reticulum and targets it to the Golgi. Cold Spring Harb Perspect Biol 2013;5(2). pii: a013367. doi: 10.1101/cshperspect.a013367.

20. Bednarek SY, Ravazzola M, Hosobuchi M, Amherdt M, Perrelet A, Schekman R, Orci L. COPI- and COPII-coated vesicles bud directly from the endoplasmic reticulum in yeast. Cell 1995;83:1183–1196.
21. Martínez-Menárguez JA, Geuze HJ, Slot JW, Klumperman J. Vesicular tubular clusters between the ER and Golgi mediate concentration of soluble secretory proteins by exclusion from COPI-coated vesicles. Cell 1999;98:81–90.
22. Sato K, Nakano A. Mechanisms of COPII vesicle formation and protein sorting. FEBS Lett 2007;581:2076–2082.
23. Peng R, Grabowski R, De Antoni A, Gallwitz D. Specific interaction of the yeast cis-Golgi syntaxin Sed5p and the coat protein complex II component Sec24p of endoplasmic reticulum-derived transport vesicles. Proc Natl Acad Sci U S A 1999;96:3751–3756.
24. Springer S, Schekman R. Nucleation of COPII vesicular coat complex by endoplasmic reticulum to Golgi vesicle SNAREs. Science 1998;281:698–700.
25. Kappeler F, Klopfenstein DR, Foguet M, Paccaud JP, Hauri HP. The recycling of ERGIC-53 in the early secretory pathway. ERGIC-53 carries a cytosolic endoplasmic reticulum-exit determinant interacting with COPII. J Biol Chem 1997;272:31801–31808.
26. Nishimura N, Balch WE. A di-acidic signal required for selective export from the endoplasmic reticulum. Science 1997;277:556–558.
27. Barlowe C. Signals for COPII-dependent export from the ER: what's the ticket out? Trends Cell Biol 2003;13:295–300.
28. Mancias JD, Goldberg J. The transport signal on Sec22 for packaging into COPII-coated vesicles is a conformational epitope. Mol Cell 2007;26:403–414.
29. Miller E, Antonny B, Hamamoto S, Schekman R. Cargo selection into COPII vesicles is driven by the Sec24p subunit. EMBO J 2002;21:6105–6113.
30. Miller EA, Beilharz TH, Malkus PN, Lee MC, Hamamoto S, Orci L, Schekman R. Multiple cargo binding sites on the COPII subunit Sec24p ensure capture of diverse membrane proteins into transport vesicles. Cell 2003;114:497–509.
31. Mossessova E, Bickford LC, Goldberg J. SNARE selectivity of the COPII coat. Cell 2003;114:483–495.
32. Mancias JD, Goldberg J. Structural basis of cargo membrane protein discrimination by the human COPII coat machinery. EMBO J 2008;27:2918–2928.
33. Sucic S, El-Kasaby A, Kudlacek O, Sarker S, Sitte HH, Marin P, Freissmuth M. The serotonin transporter is an exclusive client of the coat protein complex II (COPII) component SEC24C. J Biol Chem 2011;286:16482–16490.
34. Rothman JE, Wieland FT. Protein sorting by transport vesicles. Science 1996;272:227–234.
35. Sevier CS, Weisz OA, Davis M, Machamer CE. Efficient export of the vesicular stomatitis virus G protein from the endoplasmic reticulum requires a signal in the cytoplasmic tail that includes both tyrosine-based and di-acidic motifs. Mol Biol Cell 2000;11:13–22.
36. Dong C, Nichols CD, Guo J, Huang W, Lambert NA, Wu G. A triple Arg motif mediates alpha(2) (B)-adrenergic receptor interaction with Sec24C/D and export. Traffic 2012;13:857–868.
37. Hurtley SM, Helenius A. Protein oligomerization in the endoplasmic reticulum. Annu Rev Cell Biol 1989;5:277–307.
38. Sato K, Nakano A. Oligomerization of a cargo receptor directs protein sorting into COPII-coated transport vesicles. Mol Biol Cell 2003;14:3055–3063.
39. Zheng C, Liu HH, Yuan S, Zhou J, Zhang B. Molecular basis of LMAN1 in coordinating LMAN1-MCFD2 cargo receptor formation and ER-to-Golgi transport of FV/FVIII. Blood 2010;116:5698–5706.
40. Nourse MB, Rolle MW, Pabon LM, Murry CE. Selective control of endothelial cell proliferation with a synthetic dimerizer of FGF receptor-1. Lab Invest 2007;87:828–835.
41. Dolinski K, Muir S, Cardenas M, Heitman J. All cyclophilins and FK506 binding proteins are, individually and collectively, dispensable for viability in *Saccharomyces cerevisiae*. Proc Natl Acad Sci U S A 1997;94:13093–13098.
42. Clackson T, Yang W, Rozamus LW, Hatada M, Amara JF, Rollins CT, Stevenson LF, Magari SR, Wood SA, Courage NL, Lu X, Cerasoli F Jr, Gilman M, Holt DA. Redesigning an FKBP-ligand interface to generate chemical dimerizers with novel specificity. Proc Natl Acad Sci U S A 1998;95:10437–10442.
43. Johnson LM, Bankaitis VA, Emr SD. Distinct sequence determinants direct intracellular sorting and modification of a yeast vacuolar protease. Cell 1987;48:875–885.
44. Gaynor EC, te Heesen S, Graham TR, Aebi M, Emr SD. Signal-mediated retrieval of a membrane protein from the Golgi to the ER in yeast. J Cell Biol 1994;127:653–665.
45. Nakamura N, Yamazaki S, Sato K, Nakano A, Sakaguchi M, Mihara K. Identification of potential regulatory elements for the transport of Emp24p. Mol Biol Cell 1998;9:3493–3503.
46. Feuermann M, de Montigny J, Potier S, Souciet JL. The characterization of two new clusters of duplicated genes suggests a 'Lego' organization of the yeast *Saccharomyces cerevisiae* chromosomes. Yeast 1997;13:861–869.
47. Heiman MG, Walter P. Prm1p, a pheromone-regulated multispanning membrane protein, facilitates plasma membrane fusion during yeast mating. J Cell Biol 2000;151:719–730.
48. Sandmann T, Herrmann JM, Dengjel J, Schwarz H, Spang A. Suppression of coatomer mutants by a new protein family with COPI and COPII binding motifs in *Saccharomyces cerevisiae*. Mol Biol Cell 2003;14:3097–3113.
49. Crabtree GR, Schreiber SL. Three-part inventions: intracellular signaling and induced proximity. Trends Biochem Sci 1996;21:418–422.
50. Wurie HR, Buckett L, Zammit VA. Evidence that diacylglycerol acyltransferase 1 (DGAT1) has dual membrane topology in the endoplasmic reticulum of HepG2 cells. J Biol Chem 2011;286:36238–36247.
51. Bogdanov M, Dowhan W. Lipid-dependent generation of dual topology for a membrane protein. J Biol Chem 2012;287:37939–37948.
52. Kolbusz MA, Slotboom DJ, Lolkema JS. Role of individual positive charges in the membrane orientation and activity of transporters of the small multidrug resistance family. Biochemistry 2012;51:8867–8876.

53. Vitrac H, Bogdanov M, Dowhan W. In vitro reconstitution of lipid-dependent dual topology and postassembly topological switching of a membrane protein. Proc Natl Acad Sci U S A 2013;110:9338–9343.
54. Kolling R, Hollenberg CP. The ABC-transporter Ste6 accumulates in the plasma membrane in a ubiquitinated form in endocytosis mutants. EMBO J 1994;13:3261–3271.
55. Otte S, Barlowe C. Sorting signals can direct receptor-mediated export of soluble proteins into COPII vesicles. Nat Cell Biol 2004;6:1189–1194.
56. Belden WJ, Barlowe C. Role of Erv29p in collecting soluble secretory proteins into ER-derived transport vesicles. Science 2001;294:1528–1531.
57. Julius D, Schekman R, Thorner J. Glycosylation and processing of prepro-alpha-factor through the yeast secretory pathway. Cell 1984;36:309–318.
58. Wolfger H, Mamnun YM, Kuchler K. Fungal ABC proteins: pleiotropic drug resistance, stress response and cellular detoxification. Res Microbiol 2001;152(3–4):375–389.
59. Fiedler K, Veit M, Stamnes MA, Rothman JE. Bimodal interaction of coatomer with the p24 family of putative cargo receptors. Science 1996;273:1396–1399.
60. Ellgaard L, Molinari M, Helenius A. Setting the standards: quality control in the secretory pathway. Science 1999;286:1882–1888.
61. Christis C, Lubsen NH, Braakman I. Protein folding includes oligomerization – examples from the endoplasmic reticulum and cytosol. FEBS J 2008;275:4700–4727.
62. Gardner TG, Kearse KP. Modification of the T cell antigen receptor (TCR) complex by UDP-glucose:glycoprotein glucosyltransferase. TCR folding is finalized convergent with formation of alpha beta delta epsilon gamma epsilon complexes. J Biol Chem 1999;274:14094–14099.
63. Copeland CS, Doms RW, Bolzau EM, Webster RG, Helenius A. Assembly of influenza hemagglutinin trimers and its role in intracellular transport. J Cell Biol 1986;103:1179–1191.
64. Appenzeller C, Andersson H, Kappeler F, Hauri HP. The lectin ERGIC-53 is a cargo transport receptor for glycoproteins. Nat Cell Biol 1999;1:330–334.
65. Nufer O, Kappeler F, Guldbrandsen S, Hauri HP. ER export of ERGIC-53 is controlled by cooperation of targeting determinants in all three of its domains. J Cell Sci 2003;116:4429–4440.
66. Kreis TE, Lodish HF. Oligomerization is essential for transport of vesicular stomatitis viral glycoprotein to the cell surface. Cell 1986;46:929–937.
67. Sitte HH, Farhan H, Javitch JA. Sodium-dependent neurotransmitter transporters: oligomerization as a determinant of transporter function and trafficking. Mol Interv 2004;4:38–47.
68. Abe M, Hashimoto H, Yoda K. Molecular characterization of Vig4/Vrg4 GDP-mannose transporter of the yeast *Saccharomyces cerevisiae*. FEBS Lett 1999;458:309–312.
69. Gao XD, Dean N. Distinct protein domains of the yeast Golgi GDP-mannose transporter mediate oligomer assembly and export from the endoplasmic reticulum. J Biol Chem 2000;275:17718–17727.
70. Otte S, Barlowe C. The Erv41p-Erv46p complex: multiple export signals are required in trans for COPII-dependent transport from the ER. EMBO J 2002;21:6095–6104.
71. Franke M, Braulke T, Storch S. Transport of the GlcNAc-1-phosphotransferase alpha/beta-subunit precursor protein to the Golgi apparatus requires a combinatorial sorting motif. J Biol Chem 2013;288:1238–1249.
72. Farhan H, Freissmuth M, Sitte HH. Oligomerization of neurotransmitter transporters: a ticket from the endoplasmic reticulum to the plasma membrane. Handb Exp Pharmacol 2006;175:233–249.
73. Farhan H, Reiterer V, Korkhov VM, Schmid JA, Freissmuth M, Sitte HH. Concentrative export from the endoplasmic reticulum of the gamma-aminobutyric acid transporter 1 requires binding to SEC24D. J Biol Chem 2007;282:7679–7689.
74. Yuan H, Michelsen K, Schwappach B. 14-3-3 Dimers probe the assembly status of multimeric membrane proteins. Curr Biol 2003;13:638–646.
75. Majoul IV, Onichtchouk D, Butkevich E, Wenzel D, Chailakhyan LM, Duden R. Limiting transport steps and novel interactions of Connexin-43 along the secretory pathway. Histochem Cell Biol 2009;132:263–280.
76. Letourneur F, Hennecke S, Démollière C, Cosson P. Steric masking of a dilysine endoplasmic reticulum retention motif during assembly of the human high affinity receptor for immunoglobulin E. J Cell Biol 1995;129:971–978.
77. Blagoveshchenskaya A, Cheong FY, Rohde HM, Glover G, Knödler A, Nicolson T, Boehmelt G, Mayinger P. Integration of Golgi trafficking and growth factor signaling by the lipid phosphatase SAC1. J Cell Biol 2008;180:803–812.
78. Delgado P, Alarcon B. An orderly inactivation of intracellular retention signals controls surface expression of the T cell antigen receptor. J Exp Med 2005;201:555–566.
79. Shenkman M, Ehrlich M, Lederkremer GZ. Masking of an endoplasmic reticulum retention signal by its presence in the two subunits of the asialoglycoprotein receptor. J Biol Chem 2000;275:2845–2851.
80. McMahon HT, Gallop JL. Membrane curvature and mechanisms of dynamic cell membrane remodelling. Nature 2005;438:590–596.
81. Domanov YA, Aimon S, Toombes GE, Renner M, Quemeneur F, Triller A, Turner MS, Bassereau P. Mobility in geometrically confined membranes. Proc Natl Acad Sci U S A 2011;108:12605–12610.
82. Aimon S, Manzi J, Schmidt D, Poveda Larrosa JA, Bassereau P, Toombes GE. Functional reconstitution of a voltage-gated potassium channel in giant unilamellar vesicles. PLoS One 2011;6:e25529.
83. Dykstra ML, Cherukuri A, Pierce SK. Floating the raft hypothesis for immune receptors: access to rafts controls receptor signaling and trafficking. Traffic 2001;2:160–166.
84. Baird B, Sheets ED, Holowka D. How does the plasma membrane participate in cellular signaling by receptors for immunoglobulin E? Biophys Chem 1999;82(2–3):109–119.
85. Mellman I. Endocytosis and molecular sorting. Annu Rev Cell Dev Biol 1996;12:575–625.
86. Gagescu R, Demaurex N, Parton RG, Hunziker W, Huber LA, Gruenberg J. The recycling endosome of Madin-Darby canine kidney

cells is a mildly acidic compartment rich in raft components. Mol Biol Cell 2000;11:2775–2791.
87. Bi X, Corpina RA, Goldberg J. Structure of the Sec23/24-Sar1 pre-budding complex of the COPII vesicle coat. Nature 2002;419:271–277.
88. Peter BJ, Kent HM, Mills IG, Vallis Y, Butler PJ, Evans PR, McMahon HT. BAR domains as sensors of membrane curvature: the amphiphysin BAR structure. Science 2004;303:495–499.
89. Zimmerberg J, Kozlov MM. How proteins produce cellular membrane curvature. Nat Rev Mol Cell Biol 2006;7:9–19.
90. Copic A, Latham CF, Horlbeck MA, D'Arcangelo JG, Miller EA. ER cargo properties specify a requirement for COPII coat rigidity mediated by Sec13p. Science 2012;335:1359–1362.
91. Silvius J. Cell biology. Membrane bending tug of war. Science 2012;335:1308–1309.
92. Stachowiak JC, Brodsky FM, Miller EA. A cost-benefit analysis of the physical mechanisms of membrane curvature. Nat Cell Biol 2013;15:1019–1027.
93. Majoul I, Straub M, Hell SW, Duden R, Söling HD. KDEL-cargo regulates interactions between proteins involved in COPI vesicle traffic: measurements in living cells using FRET. Dev Cell 2001;1: 139–153.
94. Shimoni Y, Schekman R. Vesicle budding from endoplasmic reticulum. Methods Enzymol 2002;351:258–278.
95. Antonny B, Madden D, Hamamoto S, Orci L, Schekman R. Dynamics of the COPII coat with GTP and stable analogs. Nat Cell Biol 2001;3:531–537.
96. Gimeno RE, Espenshade P, Kaiser CA. COPII coat subunit interactions: Sec24p and Sec23p bind to adjacent regions of Sec16p. Mol Biol Cell 1996;7:1815–1823.
97. Sikorski RS, Hieter P. A system of shuttle vectors and yeast host strains designed for efficient manipulation of DNA in *Saccharomyces cerevisiae*. Genetics 1989;122:19–27.
98. Emr SD, Schekman R, Flessel MC, Thorner J. An MF alpha 1-SUC2 (alpha-factor-invertase) gene fusion for study of protein localization and gene expression in yeast. Proc Natl Acad Sci U S A 1983;80:7080–7084.
99. Wessel D, Flügge UI. A method for the quantitative recovery of protein in dilute solution in the presence of detergents and lipids. Anal Biochem 1984;138:141–143.